

Mechanism and Kinetics of RAFT-Based Living Radical Polymerizations of Styrene and Methyl Methacrylate

Atsushi Goto,[†] Koichi Sato,[†] Yoshinobu Tsujii,[†] Takeshi Fukuda,^{*,†} Graeme Moad,[‡] Ezio Rizzardo,[‡] and San H. Thang[‡]

Institute for Chemical Research, Kyoto University, Uji, Kyoto 611-0011, Japan, and CSIRO Molecular Science, Private Bag 10, Clayton South MDC, Clayton, Victoria 3169, Australia

Received May 30, 2000

ABSTRACT: The bulk polymerizations of styrene and methyl methacrylate in the presence of model polymer–dithiocarbonate adducts as mediators and benzoyl peroxide (BPO) as a conventional initiator were kinetically studied. The polymerization rate, and hence the concentration of polymer radical P^* , was proportional to $[BPO]^{1/2}$. The pseudo-first-order activation rate constants k_{act} were determined by the GPC peak-resolution and the polydispersity-analysis methods. The results showed that k_{act} is directly proportional to $[P^*]$, indicating that reversible addition–fragmentation chain transfer (RAFT) is the only important mechanism of activation. The magnitude of the exchange rate constant k_{ex} ($= k_{act}/[P^*]$) was strongly dependent on both the structures of the dithiocarbonate group and the polymer. The k_{ex} values for the three RAFT systems examined in this work were all very large, which explains why these systems can provide low-polydispersity polymers from an early stage of polymerization. The activation energy of k_{ex} for a polystyryl dithioacetate (PSt–SCSCH₃) was 21.0 kJ mol^{−1}, which is reasonable for a fast addition reaction.

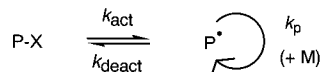
Introduction

There has recently been a surge of interest in living radical polymerization techniques as new and facile synthetic routes to well-defined, low-polydispersity polymers.^{1–6} Mechanistically, these techniques are based on the common concept of alternating activation–deactivation processes (Scheme 1a), in which a potentially active (dormant) species $P-X$ is reversibly activated to the reactive radical P^* by thermal, photochemical, and/or chemical stimuli. In the presence of monomer M , P^* propagates with a mean rate $k_p[M]$ until it is deactivated by a capping agent X , where k_p is the rate constant of propagation. A number of activation–deactivation cycles allow all the chains to have an almost equal opportunity to grow, leading to low-polydispersity polymers (when other reactions are relatively unimportant). This means that the frequency of such cycles, i.e., the magnitude of the activation rate constant k_{act} , fundamentally characterizes the performance of a given living radical polymerization.

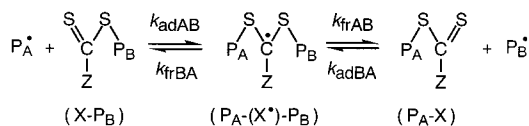
The CSIRO group has recently developed a novel living radical polymerization using dithio compounds (Scheme 1b: e.g., $X = -SCSCH_3$ and $-SCSPh$).^{7–11} The mechanism of activation presumably involves a reversible addition–fragmentation chain transfer (RAFT: Scheme 1b) process. The low polydispersities ($M_w/M_n < 1.1$) of the polymers produced in this polymerization even at an early stage of polymerization^{7–11} indicate that these RAFT processes are extremely fast. In this work, we have determined the k_{act} for the RAFT-based polymerizations of styrene (St) and methyl methacrylate (MMA) as a function of polymerization rate R_p and temperature T . In this way, we were able to establish the activation mechanism of these systems and present well-defined experimental data on the relevant rate constant and its activation energy.

Scheme 1. (a) General Scheme of Reversible Activation, (b) RAFT, (c) Degenerative Chain Transfer, and (d) Dissociation–Combination

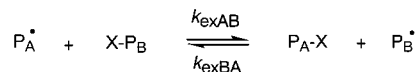
(a) General scheme of reversible activation



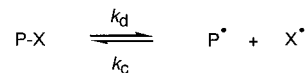
(b) RAFT ($Z = CH_3$ or Ph)



(c) Degenerative chain transfer



(d) Dissociation–combination



Experimental Section

Materials. St (99%, Wako Pure Chemical, Japan), MMA (99%, Nacalai Tesque, Japan), benzene (99.5%, Nacalai), benzoyl peroxide (BPO, 75% containing 25% water, Nacalai), and azobis(isobutyronitrile) (AIBN, 98%, Wako) were purified by distillation or recrystallization, as described previously.¹² 1-Phenylethyl dithioacetate (**1**), 1-phenylethyl dithiobenzoate (**2**), and 2-phenylprop-2-yl dithiobenzoate (**3**) were prepared according to the published procedure.⁷

Gel Permeation Chromatography (GPC). The GPC analysis was made on a Tosoh HLC-802 UR high-speed liquid chromatograph equipped with Tosoh gel columns G2500H, G3000H, and G4000H (Tokyo, Japan). Tetrahydrofuran (THF) was used as eluent (40 °C). The column system was calibrated with Tosoh standard polystyrenes (PSts). Sample detection and

[†] Kyoto University.

[‡] CSIRO Molecular Science.

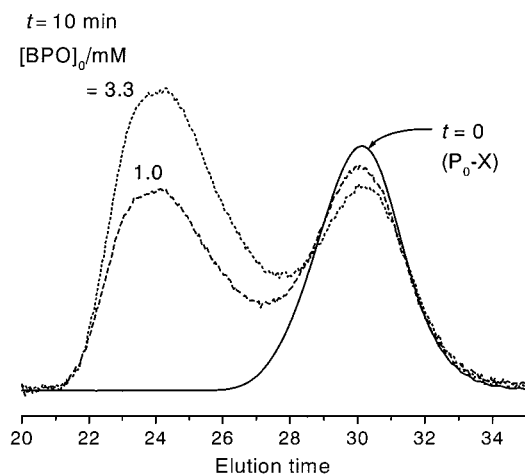


Figure 1. Examples of GPC chromatograms of the raw polymerization products in the St/PSt-SCSCH₃(P₀-X) system (60 °C): [P₀-X]₀ = 0.45 mM; [BPO]₀ as indicated in the figure.

quantification were made with a Tosoh differential refractometer RI-8020 calibrated with known concentrations of PSTs in THF.

Preparation of Polymer-Dithiocarbonates. A St solution of **1** (17 mM) and BPO (10 mM) in a glass tube was degassed by several freeze-thaw-pump cycles, sealed off under vacuum, and heated at 60 °C for 3 h. After purification,¹³ there was isolated a polystyryl dithioacetate (PSt-SCSCH₃), which, according to GPC, had number- and weight-average molecular weights M_n and M_w of 1.94×10^3 and 2.31×10^3 , respectively ($M_w/M_n = 1.17$). A chain extension test¹⁴ showed that this polymer contains 6% ($f_{\text{dead}} = 0.06$) of potentially inactive species (without dithioacetate moiety at the chain end). Similarly, a St solution of **2** (41 mM) and BPO (7.5 mM) was heated at 80 °C for 3.5 h, giving a polystyryl dithiobenzoate (PSt-SCSPh) with $M_n = 1.99 \times 10^3$, $M_w/M_n = 1.07$, and $f_{\text{dead}} = 0.06$. A MMA/benzene (3/1 v/v) solution of **3** (145 mM) and AIBN (30 mM) provided, after heat treatment at 60 °C for 7.5 h, a PMMA-dithiobenzoate (PMMA-SCSPh) with $M_n = 1.67 \times 10^3$, $M_w/M_n = 1.20$, and $f_{\text{dead}} = 0.01$.

Kinetic Analysis of Polymerization. The polymeric dithiocarbonates described above were used as probe adducts P₀-Xs. P₀-X and BPO were dissolved in monomer (St or MMA), degassed, sealed off under vacuum, and heated at a prescribed temperature for a prescribed time t . The reaction mixture was diluted by THF to a known concentration and analyzed by GPC.

Results and Discussion

Before presenting the results of experiments, we should note that most experiments given in this work are so designed as to determine k_{act} with the highest possible accuracy. Accordingly, *the experimental conditions in this work are quite different from those in the usual work* which aims at the preparation of low-polydispersity, well-defined polymers.

Polymerization Rate of St/Polystyryl Dithioacetate (PSt-SCSCH₃)/BPO System. We first examine the polymerization of St including a fixed amount of PSt-SCSCH₃ (0.45 mM) as a probe P₀-X and variable amounts of BPO (0–10 mM) as a radical initiator. Figure 1 shows examples of the GPC curves for the mixtures heated at 60 °C for $t = 10$ min. Since a constant volume of sample solution was injected to the GPC system in all runs, the total area under each curve relative to that of the $t = 0$ curve shows the amount of the monomer converted to polymer. An independent experiment confirmed that the GPC RI (refractive index) detector responses of PSt-SCSCH₃s do not depend on

Table 1. Values of $\ln([M]_0/[M])$, $\ln(S_0/S)$, Y_B , and $2[Y_B - (1/x_{n,B})]^{-1}$ for the St/PSt-SCSCH₃(P₀-X)/BPO System^a (60 °C)

[BPO] ₀ /mM	t /min	$\ln([M]_0/[M])^b$	$\ln(S_0/S)^c$	Y_B	$2[Y_B - (1/x_{n,B})]^{-1}^d$
0	60	0.0012	0.15	9.57	0.21
	120	0.0027	0.45	3.93	0.51
	180	0.0042	0.54	2.93	0.68
	240	0.0054	0.82	2.24	0.89
	300	0.0070	1.10	1.67	1.20
1.0	10	0.0011	0.16	11.8	0.17
	20	0.0021	0.28	6.39	0.31
	30	0.0030	0.48	4.18	0.48
	40	0.0040	0.61	3.07	0.65
	50	0.0050	0.85	2.22	0.90
3.0	5	0.0009	0.11	18.1	0.11
	10	0.0017	0.26	8.10	0.25
	15	0.0025	0.41	4.68	0.43
	20	0.0034	0.60	3.49	0.58
	25	0.0044	0.79	2.53	0.80
10	30	0.0051	0.93	2.17	0.93
	6	0.0016	0.15	7.89	0.25
	9	0.0025	0.34	4.46	0.45
	12	0.0033	0.46	3.45	0.59
	15	0.0043	0.64	2.54	0.79
	18	0.0052	0.90	2.11	0.96

^a [P₀-X]₀ = 0.45 mM. ^b Plot of $\ln([M]_0/[M])$ vs t is shown in Figure 2. ^c Plot of $\ln(S_0/S)$ vs t is shown in Figure 4. ^d Plot of $2[Y_B - (1/x_{n,B})]^{-1}$ vs t is shown in Figure 6.

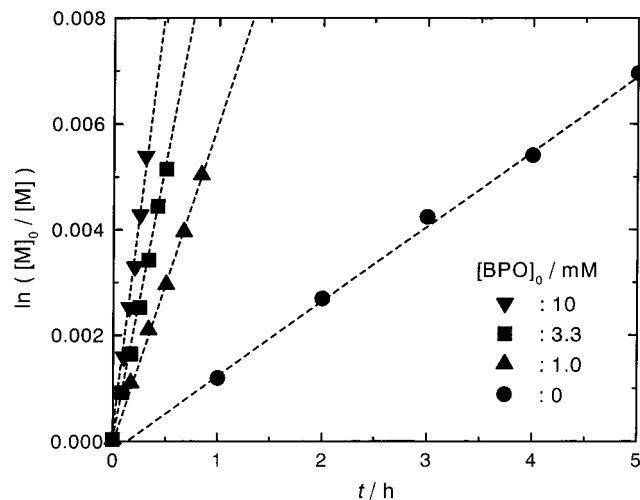


Figure 2. Plot of $\ln([M]_0/[M])$ vs t (60 °C) for the St/PSt-SCSCH₃(P₀-X) system: [P₀-X]₀ = 0.45 mM; [BPO]₀ as indicated in the figure.

chain length and agree with those of standard PSTs within 1 or 2% in the studied range of molecular weights ($M_n \geq 1600$). Numerical data of the polymerizations are summarized in Table 1.

Figure 2 shows the first-order plot of the monomer concentration $[M]$. In the studied range of conversions, the plot is approximately linear, indicating that the system is in a stationary state with respect to the ratio $R_p/[M]$ ($= k_p[P^*]$). There was a few minutes of induction period when [BPO]₀ was zero. This system showed a nonzero value of R_p due to the spontaneous (thermal) initiation of styrene. This rate, however, was so small at 60 °C (see the ordinate scale in Figure 2) that even a usually unimportant amount of impurity seems to have brought about the detectable induction period.

Figure 3 shows the plot of $(R_p/[M])^2$ vs [BPO]₀, which confirms that $[P^*]^2$ is linear to [BPO]₀. In this regard, the RAFT process has no effect on R_p , as is usually the case with the polymerizations with a conventional chain transfer agent. However, independent experiments carried out with [BPO]₀ = 6 mM showed that the R_p s of the RAFT systems with [PSt-SCSCH₃]₀ = 0.45 and 4.5

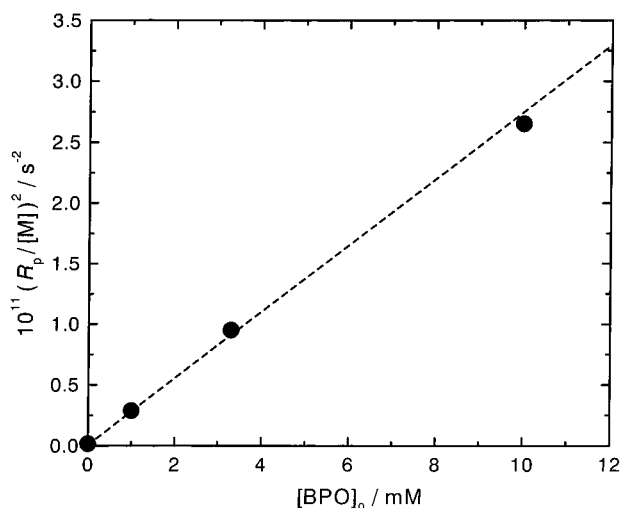


Figure 3. Plot of $(R_p/[M])^2$ vs $[BPO]_0$ (60 °C) for the St/PSt-SCSCH₃(P₀-X) system: $[P_0-X]_0 = 0.45$ mM.

mM are about 5% and about 20%, respectively, smaller than that of the conventional (RAFT agent free) system. This rather weak dependence of R_p on the RAFT agent concentration suggests that a possible reason for this may be the chain length dependence of the termination rate constant k_t ; as we previously showed,^{5,6} in any variant of living radical polymerization with a sufficiently large rate R_i of (conventional) initiation, the stationary state is eventually reached in a predictable time after the onset of polymerization, where the system follows the conventional rate law shown in eq 1.

$$R_p = (k_p/k_t^{1/2})R_i^{1/2}[M] \quad (1)$$

Since the number-average chain length x_n in living polymerization at a given conversion is inversely proportional to the concentration of living chains or the concentration of the initiating adduct P₀-X, and since k_t varies with x_n as $k_t \propto x_n^{-m}$ with $m = 0.15-0.2$,¹⁵ the observed dependence of R_p on the RAFT agent concentration may possibly be ascribed to the chain length dependence of k_t . In the St/polystyryl iodide (PSt-I)/BPO system studied previously,¹⁶ a degenerative transfer-type system, such dependence of R_p on the PSt-I concentration was not observed, even though the experiments were made for only one concentration of the PSt-I. Presumably, the chain length difference between the iodide and iodide-free systems studied in this case happened to be small so that the mentioned dependence of k_t was unimportant.

Determination of k_{act} for the St/PSt-SCSCH₃ System. The activation rate constant k_{act} was first determined by the GPC peak resolution method.¹⁷ This method is based on the GPC observation of an early stage of the polymerization containing P₀-X. When P₀-X is activated, the released P₀[•] will propagate until it is deactivated to give a new adduct P₁-X. Since P₀-X and P₁-X are generally different in chain length and its distribution, they may be distinguishable by GPC. By following the change in $[P_0-X]$, k_{act} can be determined from the first-order plot

$$\ln(S_0/S) = k_{act}t \quad (2)$$

where S_0 and S are the concentrations (or the GPC peak areas) of P₀-X at times zero and t , respectively. A lower

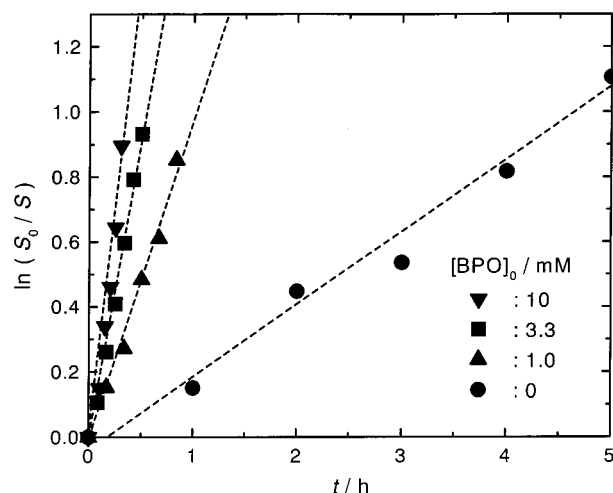


Figure 4. Plot of $\ln(S_0/S)$ vs t (60 °C) for the St/PSt-SCSCH₃(P₀-X) system: $[P_0-X]_0 = 0.45$ mM; $[BPO]_0$ as indicated in the figure.

initial concentration of P₀-X leads to a larger number of monomer units added to P₀[•] during an activation-deactivation cycle.¹⁶ In fact, with a sufficiently low $[P_0-X]_0$ (0.45 mM), the GPC curves were composed of two definite peaks such as shown in Figure 1, thus allowing accurate resolution. The lower molecular weight component corresponds to the unreacted P₀-X, and the higher molecular weight one corresponds to P₁-X (plus other minor components such as those originated from BPO). Figure 4 shows the plot of $\ln(S_0/S)$ vs t for various concentrations of BPO. The plot is linear in all cases, giving a well-defined value of k_{act} . (A short induction period is observed for $[BPO]_0 = 0$; see above.) Since P₀-X originally contains 6% of potentially inactive species (without the dithioacetate moiety; see the Experimental Section), the data have been corrected by subtracting $0.06S_0$ from both S_0 and S in eq 2. The primary oxygen-centered radical generated from BPO (PhCOO[•]) possibly attacks (or adds to) the C=S moiety. However, the concentration $[PhCOO^{\bullet}]$ is estimated to be much far smaller than $[P^{\bullet}]$ ($[PhCOO^{\bullet}]/[P^{\bullet}] \approx 10^{-3}$), and therefore the mentioned reaction should be totally unimportant. The k_{act} that we measure would be, in a most general sense, dependent on the concentration of RAFT agent, $[P_0-X]$, since it is consumed in a process which is an equilibrium. The rate of consumption becomes first order as long as the activated species P₀[•] reacts with monomer faster than it reacts with RAFT agent to be deactivated back to the starting species P₀-X. In our experimental conditions, this clearly is the case. (See Figure 1, which shows that the activated species undergoes the addition of 200 monomers on average before the deactivation. We note again that the present experimental conditions are different from the usual ones designed to obtain well-defined polymers.)

An alternative approach of k_{act} determination (the "indirect method"¹⁸) is based on the analysis of the change of polydispersities at an early stage of polymerization. We use the following simple relations that are valid for "ideal" living radical polymerizations in which reactions other than activation, deactivation, and propagation are absent and $[P^{\bullet}]$ is constant.

$$Y = w_A^2 Y_A + w_B^2 Y_B \quad (3)$$

$$F(C)[Y_B - (1/x_{n,B})]^{-1} = k_{act}t \quad (4)$$

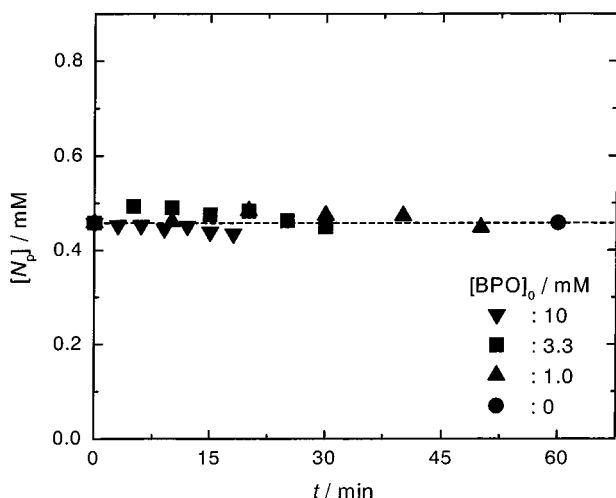


Figure 5. Plot of the number density $[N_p]$ of polymer vs t (60 °C) for the St/PSt-SCSCH₃(P₀-X) system: $[N_p]_0 = [P_0-X]_0 = 0.45$ mM; $[BPO]_0$ as indicated in the figure.

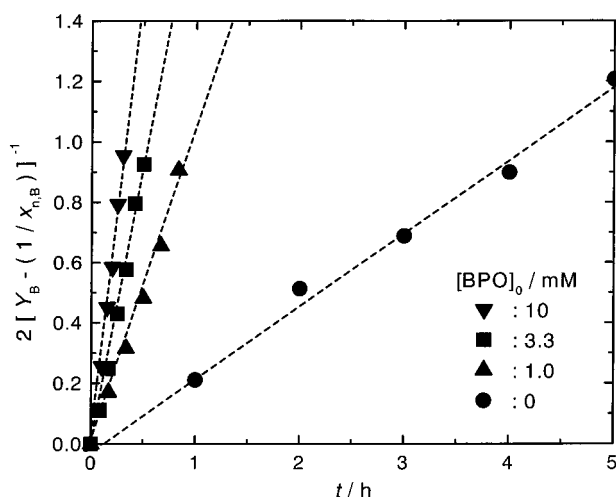


Figure 6. Plot of $2[Y_B - (1/x_{n,B})]^{-1}$ vs t (60 °C) for the St/PSt-SCSCH₃(P₀-X) system: $[P_0-X]_0 = 0.45$ mM; $[BPO]_0$ as indicated in the figure.

Here the product polymer at time t is viewed as an A-B block copolymer with the subchains A and B referring to P₀-X and the incremental part of the molecule, respectively; $Y = (x_w/x_n) - 1$, $Y_K = (x_{w,K}/x_{n,K}) - 1$, $w_A = 1 - w_B = x_{n,A}/x_n$, $x_n = x_{n,A} + x_{n,B}$, and x_n and x_w are the number- and weight-average degrees of polymerization ($K = A$ or B); the function $F(C)$ of monomer conversion C is given by $F(C) = (1 - 2C^{-1}) \ln(1 - C)$ for a batch polymerization,^{18,19} and $F(C) = 2$ for a constant-[M] system. Since we can measure the overall degrees of polymerization (x_n and x_w) and those of the subchain A ($x_{n,A}$ and $x_{w,A}$), we can calculate $x_{n,B}$ and Y_B according to eq 3 and then determine k_{act} according to eq 4. Prerequisites for this method to be valid are the constancy of both $[P^*]$ (hence $R_p/[M]$) and the number of polymer chains N_p . The $[N_p]$ estimated by the conversion C and the overall x_n was nearly constant and exceeded in no case about 8% of $[P_0-X]_0$ (Figure 5). This, coupled with the linear plot in Figure 2, confirms that the constancy of both N_p and $[P^*]$ is approximately met in this experiment. Figure 6 shows the plot of $F(C)[Y_B - (1/x_{n,B})]^{-1}$ vs t , where C is very small in all cases, so that $F(C)$ was set equal to 2. The plot is almost linear, and the slope gives a well-defined value of k_{act} in all cases.

Matyjaszewski²⁰ recently noted that eq 4 provides a poorer prediction of M_w/M_n rather than the alternative equation (the function only of C ; eq 12 in ref 20). This is a misunderstanding. The relation discussed by him (eq 13 in ref 20) is eq 4 with $F(C) = 2$ (and large $x_{n,B}$). With the function $F(C)$ given above for a batch polymerization, eq 4 and eq 12 in ref 20 are equivalent. Experimentally, eq 4 is usually more easily accessible than eq 12 in ref 20.

Mechanism of Activation. Scheme 1b shows a RAFT process, which involves the addition of radical P_A^* to the adduct P_B-X (rate constant = k_{adAB}) to form the intermediate radical, followed by the fragmentation of the intermediate to release either P_A^* (rate constant = k_{frBA}) or P_B^* (rate constant = k_{frAB}). This process, viewed as an exchanging or degenerative chain transfer process, is simplified to Scheme 1c, where k_{exAB} , for example, is the rate constant of the exchange reaction and related to the rate constants in Scheme 1b according to eq 5.

$$k_{exAB} = P_{rB} k_{adAB} \quad (5)$$

Here $P_{rB} (= 1 - P_{rA})$ is the probability for the intermediate $P_A-(X^*)-P_B$ to fragmentate into P_A-X and P_B^* and is given by eq 6.

$$P_{rB} = \frac{k_{frAB}}{k_{frAB} + k_{frBA}} \quad (6)$$

When the polymer moieties P_A and P_B are kinetically identical as in homopolymerizations with sufficiently long chains, we write $k_{exAB} = k_{exBA} = k_{ex}$, $k_{adAB} = k_{adBA} = k_{ad}$, and $k_{frAB} = k_{frBA} = k_{fr}$, which gives $P_{rA} = P_{rB} = 1/2$, i.e., eq 7.

$$k_{ex} = 1/2 k_{ad} \quad (7)$$

The existence of the intermediate radicals was confirmed by ESR spectroscopy for several RAFT systems (see below).¹⁰ However, the C-S bond may possibly be cleaved by thermal homolysis (rate constant = k_d ; Scheme 1d). If this process as well as the RAFT process is important, k_{act} will take the following form:

$$k_{act} = k_d + k_{ex}[P^*] \quad (8)$$

(There is a small possibility of the degenerative chain transfer occurring directly to the C-S bond. However, this process, if any occurs, is difficult to kinetically distinguish from the RAFT process except that the former process does not accompany the intermediate radical. For this reason, we simply neglect this process for the time being.)

Figure 7 shows the plot of k_{act} against $R_p/[M]$ ($= k_p/[P^*]$). Evidently, the data points obtained by the direct method (filled circles) and the indirect method (open circles) form a straight line passing through the origin, showing that $k_d = 0$ (within the accuracy of the present analysis), and the slope of the curve gives C_{ex} ($= k_{ex}/k_p$) = 180. This result suggests that the main mechanism of activation in this system is the RAFT process rather than thermal dissociation. With the known value of k_p (340 M⁻¹ s⁻¹),²¹ k_{ex} is estimated to be 61 000 M⁻¹ s⁻¹.

One of the reviewers of this paper pointed out that, in Figure 7, the values from the indirect method are always higher than those from the direct method. We

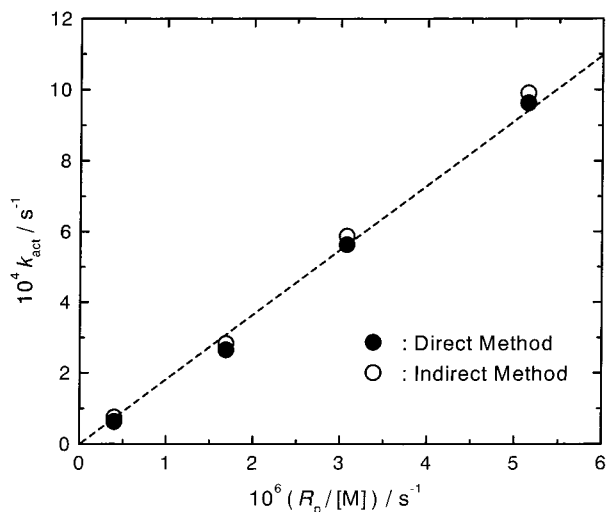


Figure 7. Plot of k_{act} vs $(R_p/[M])$ (60 °C) for the St/PSt–SCSCH₃(P₀–X) system: (●) by the direct (curve-resolution) method and (○) by the indirect (polydispersity analysis) method.

believe that this “bias” is just accidental. We previously compared the k_{act} values from the direct and indirect methods for two other system^{16,18} but observed no such trend. The trend pointed out here is within an experimental error range (about $\pm 10\%$), in any case.

A more important comment we would like to make on the indirect method refers to the Fischer theory²² given by

$$M_w/M_n = 1 + x_n^{-1} + 8/3(k_d t)^{-1} \quad (9)$$

which is valid for small t . The numerical factor $8/3$ in eq 9 should be compared to the corresponding factor 2 derived from eq 4 with $F(C) = 2$ for small t or small C . The difference is large. The Fischer system assumes the absence of initiation and the presence of termination, while the eq 4 system assumes the absence of both initiation and termination and the constant concentration of active species. In all the three systems (the present one and the other two^{16,18}) that have been experimentally studied so far, the conditions of constant $R_p/[M]$ and constant number of polymer chains, N_p , were approximately met, but both initiation and termination clearly existed. Fischer²² has commented that the extractions of rate constants using eq 9 (and eq 4) may suffer from systematic errors. We would nevertheless stress that as far as the studied three systems are concerned, the indirect method based on eq 4 (not eq 9) provided numerically consistent results to those by the direct method.

Temperature Dependence of k_{ex} for the St/PSt–SCSCH₃ System. The k_{act} values were determined by the direct method at various temperatures, all of which were carried out without BPO. Figure 8 shows the temperature dependence of k_{act} ($= k_{\text{ex}}[P^*]$) and $R_p/[M]$ ($= k_p[P^*]$). The results can be represented by eqs 10 and 11.

$$k_{\text{act}}/\text{s}^{-1} = 1.1 \times 10^7 \exp(-72.1 \text{ kJ mol}^{-1}/RT) \quad (10)$$

$$(R_p/[M])/\text{s}^{-1} = 3.6 \times 10^6 \exp(-83.6 \text{ kJ mol}^{-1}/RT) \quad (11)$$

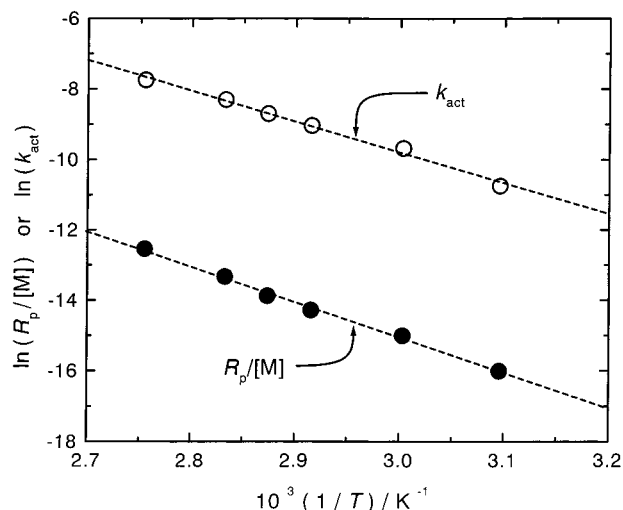


Figure 8. Plots of (○) $\ln(k_{\text{act}})$ and (●) $\ln(R_p/[M])$ vs $1/T$ for the St/PSt–SCSCH₃(P₀–X) system: $[P_0-X]_0 = 0.45 \text{ mM}$; $[BPO]_0 = 0$ at all examined temperatures.

The constant $C_{\text{ex}} (= k_{\text{ex}}/k_p)$ can be calculated with eqs 10 and 11 to give eq 12.

$$C_{\text{ex}} = 3.1 \exp(+11.5 \text{ kJ mol}^{-1}/RT) \quad (12)$$

With eq 12 and the known temperature dependence of k_p ,²¹ k_{ex} is given by eq 13.

$$k_{\text{ex}}/\text{M}^{-1} \text{ s}^{-1} = 1.3 \times 10^8 \exp(-21.0 \text{ kJ mol}^{-1}/RT) \quad (13)$$

The activation energy of 21.0 kJ mol⁻¹ is fairly small compared with those of homolytic bond cleavage reactions, e.g., the PSt–TEMPO dissociation (124 kJ mol⁻¹),¹⁷ but seems reasonable for addition reactions (k_p) such as those²¹ for St (32.51 kJ mol⁻¹) and MMA (22.34 kJ mol⁻¹) and degenerative chain transfer reactions such as that relevant to PSt–I (27.8 kJ mol⁻¹).¹⁶

St/Polystyryl Dithiobenzoate (PSt–SCSPh) System. We have also attempted to study the St polymerization with a PSt–SCSPh adduct. The k_{act} in this system was extremely large, not allowing us to determine its accurate value at this moment, but the GPC direct and indirect methods provided a crude estimate of $C_{\text{ex}} = 6000 \pm 2000$ at 40 °C. This value is about 40 times as large as the corresponding acetate value given above, demonstrating a very large effect of the ester group on the RAFT velocity.

A comment may be due regarding the large C_{ex} value estimated here. With eq 7 and the k_p value of 160 for St²¹ at 40 °C, we have $k_{\text{ad}} = 2k_{\text{ex}} = 2C_{\text{ex}}k_p \approx 1.9 \times 10^6$ (for $C_{\text{ex}} = 6000$). This value of k_{ad} is exceptionally large for an addition reaction, perhaps near the “diffusion-controlled” limit. Examples of similarly large rate constant of addition can be found in some copolymerizations. For example, the rate constant k_{12} for vinyl acetate (1)/St (2) system is estimated as $k_{12} = k_{11}/r_1 \approx 0.6 \times 10^6$ with $k_{11} = 6300$ ²³ and $r_1 = 0.01$ ²⁴ at 40 °C.

MMA/PMMA–Dithiobenzoate (PMMA–SCSPh) System. Besides the ester group, the polymer moiety would also affect the magnitude of k_{act} . We have examined the polymerization of MMA including a fixed amount of PMMA–SCSPh (P₀–X: 0.56 mM) and variable amounts of BPO (0.1–1.0 mM). BPO was added, since MMA has no appreciable spontaneous (thermal)

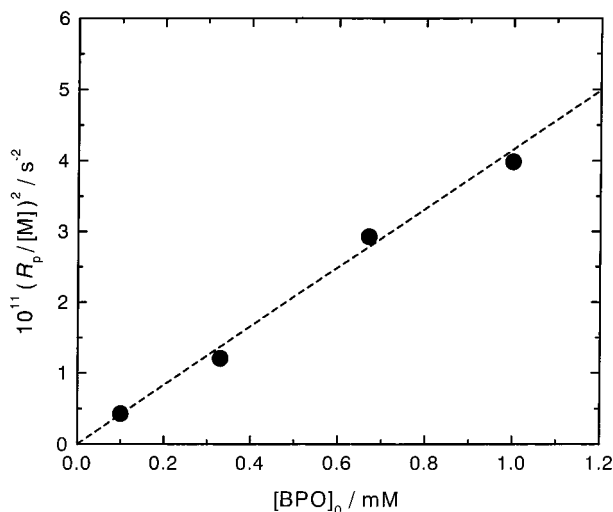


Figure 9. Plot of $(R_p/[M])^2$ vs $[BPO]_0$ (60 °C) for the MMA/PMMA-SCSPH(P_0 -X) system: $[P_0-X]_0 = 0.56$ mM.

initiation unlike St. The first-order plot of $[M]$ was approximately linear with no induction period in all examined cases (data not shown). The plot of $(R_p/[M])^2$ vs $[BPO]_0$ shown in Figure 9 confirms that $[P^\bullet]^2$ is proportional to $[BPO]_0$. The GPC chromatograms were composed of two well-separated peaks, which were used to determine k_{act} by the "direct" method. Figure 10 shows the plot of k_{act} vs $R_p/[M]$ ($= k_p[P^\bullet]$). The intercept of the straight line gives $k_d = 0$, indicating that RAFT is virtually the only mechanism of activation in the MMA system as well as in the St system. The slope of the straight line gives $C_{ex} = 140$. This value is much smaller than that for the St/PSt-SCSPH system discussed above, clearly showing that k_{act} is strongly dependent on the polymer (alkyl) moiety as well as the carbonate moiety.

Comments on the Intermediate Radicals and Block Copolymerization. Referring to Scheme 1b again, it is easy to show that the stationary-state concentration of the intermediate $P_A-(X^\bullet)-P_B$ is given by eq 14.

$$[P_A-(X^\bullet)-P_B] = \frac{k_{adAB}[P_B-X][P_A^\bullet] + k_{adBA}[P_A-X][P_B^\bullet]}{k_{frAB} + k_{frBA}} \quad (14)$$

When P_A and P_B are kinetically identical, eq 14 reduces to eq 15.

$$[P-(X^\bullet)-P] = \frac{k_{ad}}{k_{fr}}[P-X][P^\bullet] \quad (15)$$

In comparison of the St/PSt-SCSPH and MMA/PMMA-SCSPH systems, we found that $k_{ad}(St) \gg k_{ad}(MMA)$. In analogy to C-ON and C-halogen bonds, the bond energy of the PSt-SC bond will be larger than that of the PMMA-SC bond or $k_{fr}(St)$ will be smaller than $k_{fr}(MMA)$. Hence, we expect eq 16 to hold.

$$[PSt-(X^\bullet)-PSt] \gg [PMMA-(X^\bullet)-PMMA] \quad (16)$$

In fact, the intermediate radical for the St system was clearly detected by ESR, while that for the *n*-butyl methacrylate system was undetectable. This difference has been attributed to that in k_{fr} ,¹⁰ but as eq 15

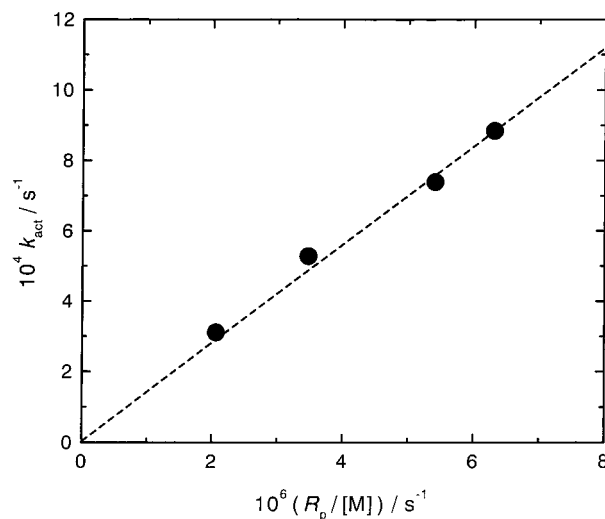


Figure 10. Plot of k_{act} vs $(R_p/[M])$ (60 °C) for the MMA/PMMA-SCSPH(P_0 -X) system: k_{act} was determined by the direct (curve-resolution) method.

indicates, the difference in k_{ad} is also important. We will come back to this point below.

Another comment concerns block copolymerization. For a smooth block copolymerization of monomer B to polymer A, for example, the exchange rate constant k_{exBA} must be large enough. We previously showed that, for a degenerative transfer-type system by a batch process, the polydispersity of the B block as a function of conversion C is given, in the ideal limit, by eq 17.

$$[Y_B - (1/x_{n,B})]^{-1} = C_{exBB}[C(2 - C)] \quad (17)$$

Let us require that $x_{n,B}^{-1} \approx 0$ and $Y_B = 0.1$ for $C = 1$, for which eq 17 gives $C_{exBB} = k_{exBB}/k_{pB} = 10$. By taking this value as a measure and referring to eq 5, the condition of smooth block copolymerization reads

$$\frac{k_{exBA}}{k_{pB}} = \frac{P_{rA}k_{adBA}}{k_{pB}} \geq 10 \quad (18)$$

Since k_{adBA} may presumably be approximated by k_{adBB} without too much error, eqs 7 and 18 give eq 19.

$$P_{rA} \geq 5C_{exBB}^{-1} \quad (19)$$

Regarding MMA/St/dithiobenzoate systems, we already know that $C_{ex}(MMA) = 140$ and $C_{ex}(St) \approx 6000$. Equation 19 obviously holds for the PSt radical adding to PMMA-X. On the other hand, in order for the PMMA radical to exchange with PSt-X, $P_r(St)$ has to be larger than about $5 \times (1/140) \approx 0.04$. The block copolymerization in this direction did not go smoothly,⁹ which suggests that $P_r(St) < 0.04$ or that $k_{fr}(MMA)$ is at least 25 times larger than $k_{fr}(St)$. Putting this and the about 20 times difference in k_{ad} (about 40 times difference in C_{ex} with $k_p(MMA)/k_p(St) = 2.4$ at 60 °C²¹) into eq 15, we estimate that the concentration of the intermediate radical in the MMA polymerization is at least 500 times smaller than that in the St polymerization, when other conditions are the same. This would explain why the intermediate radical was not observed for the methacrylate system.¹⁰

Figure 11 shows the plot indicated by eq 17 for all the data of the St/PSt-SCSCH₃ system with different BPO concentrations and hence different R_p s. In this

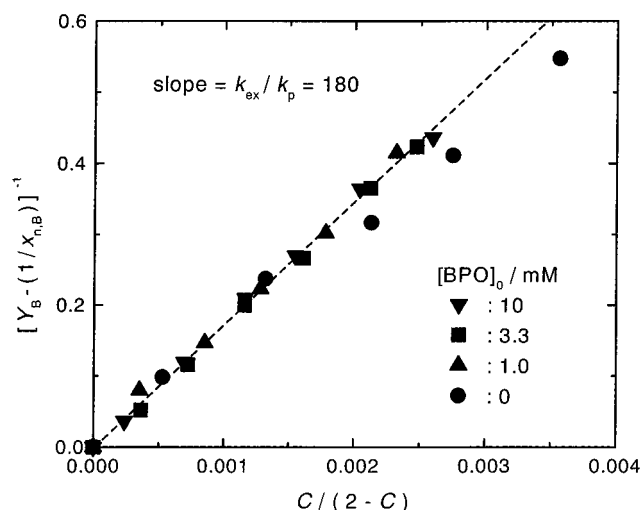


Figure 11. Plot of $[Y_B - (1/x_{n,B})]^{-1}$ vs $C/(2 - C)$ (60 °C) for the St/PSt-SCSCH₃(P₀-X) system: $[P_0-X]_0 = 0.45$ mM; $[BPO]_0$ as indicated in the figure. The three points for zero $[BPO]$ show some deviation from the line, but the deviation is ascribed to the experimental error arising from the extremely small R_p for the BPO-free system.

Table 2. Comparison of C_{ex} (60 °C)

P-X	C_{ex}
1. PSt-SCSCH ₃	180
2. PSt-SCSPh	6000 ± 2000 ^a
3. PMMA-SCSPh	140
4. PSt-I ¹⁶	4.0
5. PMMA-macromonomer ²⁵	0.20

^a Preliminary result at 40 °C.

conversion range, all the data points approximately fall on a single straight line passing through the origin with a slope of 180 ($= C_{ex}$), which naturally agrees with the value from Figure 7. Another example of such a plot, which extends to much higher conversions, has been presented elsewhere for the iodide-mediated polymerization of St.¹⁶

Conclusions

The bulk polymerizations of St and MMA in the presence of polymer-dithiocarbonate adducts and BPO were kinetically studied. The polymerization rate, and hence $[P^*]$, was proportional to $[BPO]^{1/2}$ as in the conventional (RAFT agent-free) systems. The pseudo-first-order activation rate constant, k_{act} , determined by both the GPC peak-resolution and polydispersity-analysis methods was directly proportional to $[P^*]$, meaning that the main mechanism of activation in the present systems is RAFT rather than thermal dissociation. As summarized in Table 2, the exchange rate constants C_{ex} ($= k_{ex}/k_p$) for RAFT were strongly dependent on both the structures of the dithiocarbonate group

and the polymer. In comparison with the C_{ex} values for the PSt-iodide¹⁶ and PMMA-macromonomer²⁵ systems, those for the examined RAFT systems are exceptionally large. This explains why these RAFT systems can yield low-polydispersity polymers from an early stage of polymerization.

Acknowledgment. This work was supported by a Grant-in-Aid for Scientific Research, the Ministry of Education, Science, Sports, and Culture, Japan (Grant-in-Aid 12450385), and also by Research Fellowships of the Japan Society for the Promotion of Science for Young Scientists (to A.G.).

References and Notes

- (1) Matyjaszewski, K., Ed. *ACS Symp. Ser.* **1998**, 685.
- (2) Malmström, E. E.; Hawker, C. J. *Macromol. Chem. Phys.* **1998**, 199, 923.
- (3) Matyjaszewski, K. *Chem. Eur. J.* **1999**, 5, 3095.
- (4) Sawamoto, M.; Kamigaito, M. *CHEMTECH* **1999**, 29 (6), 30.
- (5) Fukuda, T.; Goto, A.; Ohno, K. *Macromol. Rapid Commun.* **2000**, 21, 151.
- (6) Matyjaszewski, K., Ed. *ACS Symp. Ser.* **2000**, 768.
- (7) International Pat. Appl. PCT/US97/12540 WO9801478, invs.: Le, T. P. T.; Moad, G.; Rizzardo, E.; Thang, S. H. *Chem. Abstr.* **1998**, 128, 115390.
- (8) Chiefari, J.; Chong, Y. K.; Ercole, F.; Krstina, J.; Jeffery, J.; Le, T. P. T.; Mayadunne, R. T. A.; Meijs, G. F.; Moad, C. L.; Moad, G.; Rizzardo, E.; Thang, S. H. *Macromolecules* **1998**, 31, 5559.
- (9) Chong, Y. K.; Le, T. P. T.; Moad, G.; Rizzardo, E.; Thang, S. H. *Macromolecules* **1999**, 32, 2071.
- (10) Hawthorne, D. G.; Moad, G.; Rizzardo, E.; Thang, S. H. *Macromolecules* **1999**, 32, 5457.
- (11) Rizzardo, E.; Chiefari, J.; Chong, Y. K.; Ercole, F.; Krstina, J.; Jeffery, J.; Le, T. P. T.; Mayadunne, R. T. A.; Meijs, G. F.; Moad, C. L.; Moad, G.; Thang, S. H. *Macromol. Symp.* **1999**, 143, 291.
- (12) Fukuda, T.; Ma, Y.-D.; Inagaki, H. *Macromolecules* **1985**, 18, 17.
- (13) Fukuda, T.; Terauchi, T.; Goto, A.; Ohno, K.; Tsujii, Y.; Miyamoto, T.; Kobatake, S.; Yamada, B. *Macromolecules* **1996**, 29, 6393.
- (14) Goto, A.; Fukuda, T. *Macromolecules* **1997**, 30, 5183.
- (15) Olaj, O. F.; Vana, P. *Macromol. Rapid Commun.* **1998**, 19, 433.
- (16) Goto, A.; Ohno, K.; Fukuda, T. *Macromolecules* **1998**, 31, 2809.
- (17) Goto, A.; Terauchi, T.; Fukuda, T.; Miyamoto, T. *Macromol. Rapid Commun.* **1997**, 18, 673.
- (18) Fukuda, T.; Goto, A. *Macromol. Rapid Commun.* **1997**, 18, 682: the factor -2 appearing in eq 4 is a misprint for C-2.
- (19) Müller, A. H. E.; Zhuang, R.; Yan, D.; Litvinenko, G. *Macromolecules* **1995**, 28, 4326.
- (20) Matyjaszewski, K. *ACS Symp. Ser.* **2000**, 768, 2.
- (21) Gilbert, R. G. *Pure Appl. Chem.* **1996**, 68, 1491.
- (22) Fischer, H. *J. Polym. Sci., Part A: Polym. Chem.* **1999**, 37, 1885.
- (23) Ma, Y.-D.; Won, Y.-C.; Kubo, K.; Fukuda, T. *Macromolecules* **1993**, 26, 6766.
- (24) Nakata, T.; Otsu, T.; Imoto, M. *J. Polym. Sci., Part A: Polym. Chem.* **1965**, 3, 3383.
- (25) Moad, C. L.; Moad, G.; Rizzardo, E.; Thang, S. H. *Macromolecules* **1996**, 29, 7717.

MA0009451